

It's a Feature, Not a Bug!

Measuring Fluidity in Image Generators

Aditi Ramaswamy
aditi.ramaswamy@kcl.ac.uk

Melane Navaratnarajah
melane.navaratnarajah@kcl.ac.uk

Hana Chockler
hana.chockler@kcl.ac.uk

June 28, 2024

Abstract

With the rise of freely available image generators, AI-generated art has become the center of a series of heated debates, one of which concerns the concept of human creativity. Can an image generation AI exhibit “creativity” of the same type that artists do, and if so, how does that manifest? Our paper attempts to define and empirically measure one facet of creative behavior in AI, by conducting an experiment to quantify the “fluidity of prompt interpretation”, or just “fluidity”, in a series of selected popular image generators. To study fluidity, we (1) introduce a clear definition for it, (2) create chains of auto-generated prompts and images seeded with an initial "ground-truth: image, (3) measure these chains' breakage points using preexisting visual and semantic metrics, and (4) use both statistical tests and visual explanations to study these chains and determine whether the image generators used to produce them exhibit significant fluidity.

1 Introduction

There are many metrics and measures used to evaluate different aspects of image generators. However, one concept has been overlooked for a long time: creativity. This is because creativity is deeply difficult to define, let alone quantify. We aim to change this by introducing a new creativity measure to balance out the existing metric of faithfulness, which measures how strongly a generated image matches the textual prompt used to create it. Our proposed measure is “fluidity of prompt interpretation”. We measure it through building a game between auto-generated captions and images, and analyzing the results through both statistical and visual means. The proposed measure has a fine

granularity, allowing for comparison of different image generators by placing them on a scale of “fluid” to “faithful”. To the best of our knowledge, this is the first attempt at such a measure.

Related Work

Some researchers argue that creativity is derived from a “socio-cultural context”, thus excluding AI models, which “[lack]... feelings... or [the ability to] reflect” [Oppenlaender, 2022, Kaufman et al., 2019, Wingström et al., 2022]. However, other definitions focus on purely behavioral requirements, such as “domain-relevant skills”, “creativity-relevant processes”, and “extrinsic motivation”, all of which can be exhibited by generative AI models [Amabile, 1983].

A number of ethnographic studies support this. AI artists interviewed by Wingström et al. [2022] spoke of “co-creativity”, the synthesis of their own human creativity and generative AI processes, and stated that glitches in generated images are signs of creativity rather than bugs. Other studies use the Alternate Uses Task (AUT) test, an established subjective measure of creativity, to compare creative behaviors exhibited by AI chatbots and humans [Koivisto and Grassini, 2023, Haase and Hanel, 2023]. The results showed that human scorers are often unable to differentiate AI-generated results from human-generated ones. Similarly, recent research indicates that “little to no” human intervention is needed for an image generation model to produce “high-quality” art, as DALL-E can create complex and detailed pieces from very simple text prompts such as emojis or singular letters [Oppenlaender, 2022].

Using a process-oriented definition like that described by Amabile [1983], and supported by the studies conducted by Wingström et al. [2022], Koivisto and Grassini [2023], Haase and Hanel [2023], Oppenlaender [2022] we infer that some AI models may have the potential to exhibit creative behavior. This forms the motivation for our experiment.

2 Background & Experiment Construction

Here we provide definitions for fluidity and breakage point/chain length, as well as a detailed breakdown of our experimental setup, chain construction, and breakage calculation metric.

2.1 Existing Image Generation Metrics

There are a range of existing techniques for evaluating image generators which we took into consideration when creating our fluidity measure. In particular, fidelity focuses on the visual similarity between generated and ground truth images, while faithfulness evaluates the alignment between the prompt and generated images. Hu et al. [2023], for example, evaluates faithfulness in an image generation model m by leveraging an LLM to answer questions about a text prompt t given a generated image produced by t using m . This is not dissimilar

to our approach of generating images and comparing both the generated images and their captions to a predetermined “ground truth”. However, there is no definitive measure to study the opposite of faithfulness: how much *misalignment* is there between the prompt and a generated image? Knowing this misalignment level would enable a user to choose the model which best suits their end goal. Our measure uses aspects of both fidelity and faithfulness to gauge this misalignment.

2.2 Defining and Measuring Fluidity

While creativity as a concept cannot be measured, creative behavior can be experimented on to produce analyzable results. The view on glitches being indicators of creativity in Wingström et al. [2022] led us to craft an experiment to evaluate image generators for one measure of creative behavior. This measure is “fluidity of prompt interpretation”, or simply fluidity.

Definition 1 (Fluidity) *The relative extent of misalignment between the output of a given image generator and the semantics of its input prompt, placed on a scale from a hypothetical completely random image generator to a hypothetical completely faithful one, using the definition of faithfulness provided by Hu et al. [2023].*

We measure the fluidity of a given generator through constructing numerous alternating chains of generated images and captions, calculating when each chain strays too far from the original “ground truth” (a “breaking point”), and then studying the statistical properties of the ensuing distribution of chain lengths.

2.3 Computational Resources & Justifications

Due to computational limitations, we could not run each chain until its natural breaking point. We set a hard limit of 15 generated images, as that is long enough to let us tell whether a chain stays faithful to the “ground truth” image and caption, but short enough not to require more resources than we could afford. Our experiment therefore required 1000 chains of 15 generated images and 16 generated captions for 12 different image+caption generator combinations in Table 7, plus 15 generated captions for each of the control chain combinations shown in Table 8. For each combination, we used 1-2 A100 GPUs. A chain length of 15 is therefore synonymous with the chain staying unbroken.

2.4 Chain Construction

As in Chinese Whispers, each chain in our experiment begins with a “ground truth”, or seed image, pulled from `coco_1000`, a set of 1000 images which we compiled from the publicly-available, non-copyrighted COCO dataset [Lin et al., 2014]. Our compilation process involved randomly selecting photographs from COCO, while using YOLO object detection to ensure that each chosen photo had a clear subject and did not prominently feature human faces [Jocher et al., 2023]. The latter criterion is because facial features are inherently so variable

that determining an easily understandable breakage point between two facial images is too subjective.

To build a chain, we caption the initial “ground truth” seed image using one of three caption generation models from Hugging Face¹: TEXTCAPS, BLIP, and LLAVA [Wang et al., 2022, Li et al., 2022, Liu et al., 2023]. This caption is then fed into one of four open-source image generation models: OPENDALLE, KANDINSKY 2.2, STABLE-DIFFUSION, and SDXL-TURBO [Izquierdo, 2024, Razzhigaev et al., 2023, Rombach et al., 2021, Sauer et al., 2023]. To ensure determinism in our experiment, we seeded each image generator with a constant value (the caption generators are already deterministic). We also tested reproducibility by running miniature versions of our experiments for each image generator (using LLAVA) and used Mann-Whitney U tests to confirm that the chain length frequency distributions produced by each of the new experiments had no statistically significant difference from those we derived from the main experiment.

For STABLE-DIFFUSION, we added negative and positive prompt lists to ensure that the outputs to remain photo-like so they could be better compared to the “ground truth” photo[Berger et al., 2023]. We also set the guidance scale (when it was a viable parameter) to the maximum value, as we wanted to observe the fluidity of these image generation models when they are explicitly instructed to adhere to a given text prompt as much as possible.

Our reason for choosing multiple captioning models is to mitigate the effect a single captioning tool may have on the effects: if it produces inaccurate captions, it could cause the chains to break early even if the image generator is faithful in interpreting a given prompt. Using three different captioning tools balances this out by allowing us to compare the three to determine whether the captioning tool has a significant influence on chain breakage. Since image generation models tend to do best with concise prompts, we limited the maximum caption length to 50 for TEXTCAPS, and for LLAVA we requested a “concise caption” within the parameters. BLIP used default parameters, but produced captions of roughly the same length as LLAVA and TEXTCAPS.

We also created a control group of “dummy” chains to represent the products of running our experiment with a hypothetically maximally faithful, minimally fluid image generator. We determined that such a generator would produce extremely similar images at each step in the chain, sticking to the original image and prompt with extreme fidelity and faithfulness. We pulled 15 images each of “dummy” images from a Kaggle dataset of bears, zebras, and giraffes, common subjects in our input image dataset [Likhon, 2024]. To simulate the 1000 image chains produced by each of our true experiments, we randomly shuffled each set of 15 images of the same category 333 times, captioned each image as if it were a real chain, and then calculated the breaking metrics using the same formulae as the real chains. The creation of this control group was necessary in order to have a null hypothesis to which the image generators could be compared: because the images in each control chain are extremely similar, they represent the most faithful interpretations of the seed prompt, thus simulating an image generator

¹<https://huggingface.co/>

which always acts with extremely low fluidity and extremely high faithfulness.

We check whether our experimental results are statistically significant by using the Mann-Whitney U non-parametric test to compare the chain length frequency distributions of chain lengths for each image and caption generator combination with a corresponding control group distribution, and we compare fluidity levels amongst different image and caption generator combinations by using Kullback-Leibler divergence.

2.5 Image Guidance, Glitches, & Breaking Calculations

Our breakage criteria depend on the presence of generative AI glitches, caused by semantic misunderstandings between the text prompts and the embeddings of the generative models used to produce images [Chefer et al., 2023]. Often, these can result in the intended subjects from the text prompt either not being generated (“catastrophic neglect”), or being given less importance than background information from the text prompt (“incorrect attribute binding”). Examples from Chefer et al. [2023] include the prompt “a yellow bowl and a blue cat” producing blue-and-yellow bowls, and “a yellow bow and a brown bench” producing the specified items, but coloring both yellow. Computational creativity also views “incongruities” and “anomalies” such as these as *opportunities for further search*, or paths which may lead to “*surprisingly meaningful results*” [Veale et al., 2019]. This fluidity is an important aspect of creativity: humans often interpret media, such as literary works, in unexpected or unusual ways. Therefore, examining unusual semantic interpretations performed by image generators through the lens of creative, rather than buggy, behavior, can lead to new insights on the contrasts and similarities between humans’ and machines’ understanding of the world.

Definition 2 (Breaking Point/Chain Length) *The iteration x , within a given chain c , wherein img_x , the generated image at x , is too distant from the seed image’s caption s_{cap} to be considered faithful to the semantic information contained in s_{cap} . This distance is measured through Algorithm 2, which utilizes a series of preexisting metrics to determine the distance from img_x to the seed image.*

To measure chain length, we take into account multiple facets of each step in the chain, including objects found within the current generated image as well as the semantics of the current generated caption. These facets are compared to the initial seed image/caption pair using a number of metrics. Firstly, to quantify the disparities between the initial caption and each subsequent caption in the chain, we use variations of BERT to measure semantic change. Secondly, we use both CLIP and YOLO to quantify the disparities between the initial seed image and each subsequent image in the chain, by extracting the likeliest labels from each image and comparing them. Our intent in using multiple semantic scorers and object detectors is to try to mitigate any skew one particular tool may introduce into the results.

For semantic scoring, we use the ALBERT and S-BERT variations of the original BERT model [Lan et al., 2019, Reimers and Gurevych, 2019]. For ALBERT, we feed in labels representing the semantic meaning of each caption being compared: the original seed one and the caption at the current step of the chain. These labels are generated using the unsupervised keyword extraction algorithm YAKE, and if that yields no results, a second attempt at extracting labels is made using RAKE [Campos et al., 2020, Rose et al., 2010]. Both YAKE and RAKE are fast, document length-agnostic, and can extract keywords from a single document, making them ideal choices for keyword extraction from captions, which are short documents that do not belong to a larger corpus. ALBERT then uses cosine similarity to calculate the distance between the two sets of labels. S-BERT takes in the raw text for each caption, and turns it into a word embedding representation. These two embeddings are also compared using cosine similarity. Our semantic scoring metric considers the chain “broken” if the result of both metrics falls below 0.5, or a less than 50% similarity to the original caption. Example values for these metrics can be found in Table 6.

To justify this threshold, we ran a few experiments on a sample of 100 images from our `coco_1000` dataset. We determined that 0.25 is too low to produce meaningful results as almost all the chains remain unbroken, while 0.75 is too high, causing most chains to break at the first iteration.

For measuring differences in the subjects of the images, we use two object detection architectures, CLIP and YOLOWORLD [Radford et al., 2021, Cheng et al., 2024]. Torchmetrics’ CLIPSCORE is used to calculate the similarity between the current image and the initial caption, wherein a larger value means a greater difference. A threshold of 20, based on smaller experiments run beforehand, was used to determine breakage based on CLIPSCORE. Additional breakage metrics based on the images themselves were implemented using the class labels provided by both CLIP and YOLOWORLD. To compare similarity, we use algorithm $LABEL_SIM(curr_img_labels, init_img_labels)$, as defined in Algorithm 1.

Examples of object detector breakage results can be found in Table 5.

For each step x of 15 in each chain, the breakage algorithm Algorithm 2 is called in order to compare the image and caption generated at step x with the “ground truth” image and its caption which were determined at the very beginning of the chain.

Comprehensive examples of chain breakages can be found in Table 1, Table 2, Table 3, and Table 4 in the appendix.

2.6 Analysis Tools

In order to understand the underlying reasons as to why some chains broke, we used REX, an improved re-implementation of DEEPCOVER which provides visual explanations for the pre-determined ResNet152 labels applied to an input image [He et al., 2016, Chockler et al., 2022].

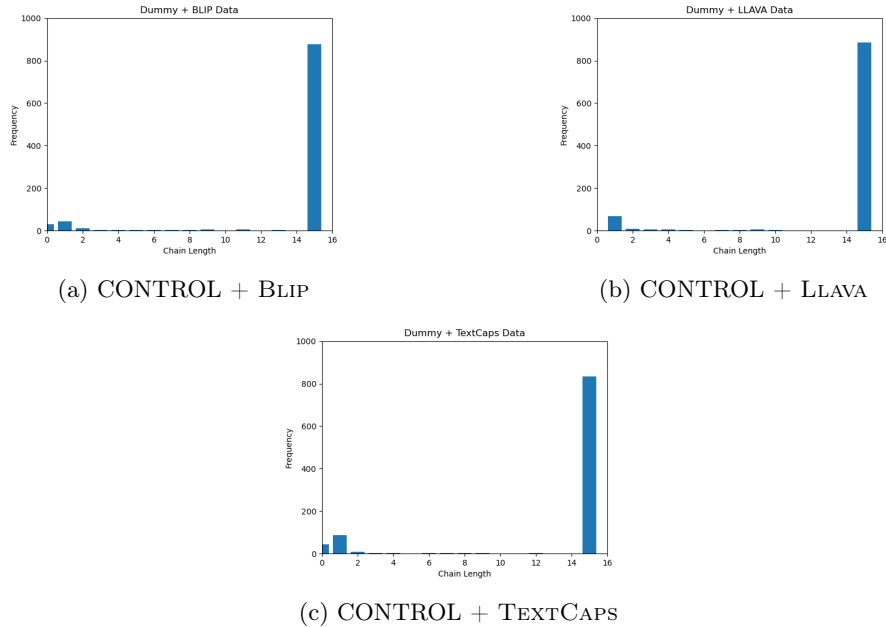


Figure 1: The chain length frequency distributions for all three control group combinations.

3 Results & Analysis

3.1 Statistical Results

To formalize our conjecture about fluidity and chain breakage, we established the following null hypothesis: *for any given combination of image generator and caption generator, the frequency distribution of chain lengths would not show a statistically significant difference from the frequency distribution of chain lengths in the control group produced with corresponding captioning tool.* The chain length frequency distributions for the control group data are shown in Figure 1.

When the frequencies of chain lengths/breakage points for each combination of image generator and caption generator were plotted, they were all negatively skewed according to the Shapiro-Wilk statistical test [Shapiro and Wilk, 1965]. Therefore, we chose to use the two-sided Mann-Whitney U non-parametric test to compare the chain data to the control group data [Mann and Whitney, 1947]. We used the implementation from the `scipy stats` library to perform both this test and KL divergence [Virtanen et al., 2020].

We performed the Mann-Whitney U test with a default p-value threshold of 0.05 on the frequency data compiled from the OPENDALLE, KANDINSKY, STABLE-DIFFUSION, and SDXL-TURBO chain outputs and the control group data corresponding to each of the caption generators BLIP, LLAVA, and TEXTCAPS.

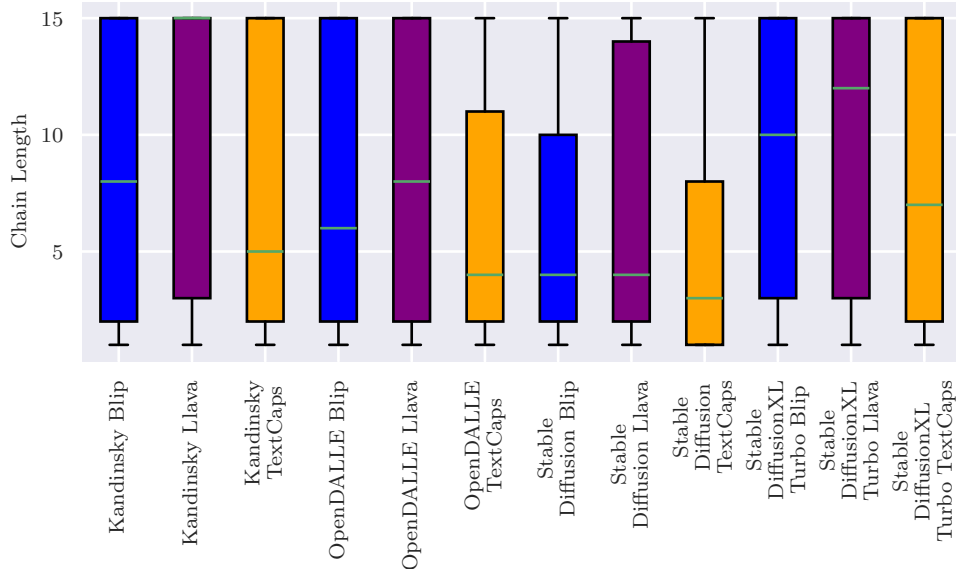


Figure 2: A box plot of the distribution of chain lengths for the different combinations of models

We also used the Mann-Whitney U test to compare image generators and captioning tools amongst themselves. In all, we performed the Mann-Whitney U test on 45 different pairs of images (see Table 9, Table 10, and Table 11), so we used the Bonferroni correction by dividing 0.05 by 45, leading to a p-value significance threshold of 0.0011 [Sedgwick, 2012].

As shown in Table 9, most of the combinations’ chain length frequency distributions differed from the expected behavior of the corresponding control groups with p-values below 0.0011. The exceptions were KANDINSKY-BLIP, KANDINSKY-TEXTCAPS, and SDXL-TURBO-TEXTCAPS.

From this, we determine that STABLE-DIFFUSION and OPENDALLE both unequivocally reject the null hypothesis that the chain length frequency distribution derived from running our experiment using a particular image generation model will not differ statistically significantly from the chain length frequency distribution derived from running our experiment using control chain data. KANDINSKY and SDXL-TURBO are ambiguous, as some of the captioning models pushed their p-values very slightly above the 0.0011 threshold while other captioning models had p-values slightly below the threshold. However, as shown in Table 11, none of the Mann-Whitney tests conducted on pairs which use the same image data and different captioning models had p-values close to the 0.0011 threshold. These results indicate that while some captioning tools may influence results slightly, the chosen captioning tool alone does not have as strong an impact on chain length frequency distributions as does the chosen image generator.

Although the Mann-Whitney U results showed no statistically significant differences between the distributions produced by the four different image generators in comparison to each other (see Table 10), the fact that a few of the image-caption generator combinations did not reject the null hypothesis meant that subtle differences did exist between different image generators. Why, for example, does STABLE-DIFFUSION-TEXTCAPS show statistically significant fluidity, while SDXL-TURBO-TEXTCAPS does not? We decided to build a quantitative scale of fluidity to faithfulness for the various combinations. To do this, we used Kullback-Leibler divergence (KL) to calculate the distance between the chain length frequency distribution for each combination and the uniform distribution. We selected the uniform distribution using the reasoning that a hypothetical image generator H_i which does not rely on semantic information at all would generate random images, representing a maximally fluid state. This unpredictability could be simulated using a uniform distribution. Figure 3 shows the KL scores for each combination when compared with the uniform distribution.

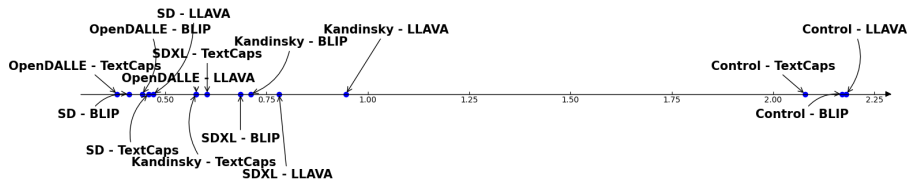


Figure 3: The different combinations of models plotted on a scale of fluidity (the direction is fluid \rightarrow faithful, with higher values representing more faithfulness) using the Kullback-Leibler divergence.

The further a combination is from the maximally fluid state, the higher its KL score will be. As can be seen here, OPENDALLE + TEXTCAPS is the closest to maximally fluid, with a KL score of 0.38, while Control + LLAVA is the furthest from maximally fluid, with a KL score of 2.18.

3.2 Analysis

Visual analysis of the outputs is integral to understanding how and why fluidity of prompt interpretation manifests within a given chain. Some chains are easy to understand at first glance, while others require more algorithmic analysis. As an example of the former case, Figure 4 shows two chains seeded with the same image, 0011, from the “ground truth” dataset. Both chains were created using BLIP for captioning, but one used the KANDINSKY model for image generation, while the other used STABLE-DIFFUSION. On the scale described in Figure 3, STABLE-DIFFUSION + BLIP has a KL score of 0.41 and is more fluid than KANDINSKY + BLIP, which has a KL score of 0.71.

The initial caption for the “ground truth” image, 0011, was “two large trucks parked next to each other on a road”. As seen in the STABLE-DIFFUSION chain, the images quickly diverged from focusing on trucks to the surrounding scenery, with the last generated image in the chain being captioned “a view of a road with trees lining both sides of it”. On the other hand, the KANDINSKY chain continues to feature trucks as the main focus, with the final generated image in the chain being captioned “several pink trucks are parked in front of a building”. The STABLE-DIFFUSION chain broke at iteration 6 due to low CLIP and YOLOWORLD label similarities between the “ground truth” seed image and the fifth generated image, while the KANDINSKY chain remained unbroken. The reasons for these chain lengths are clear: STABLE-DIFFUSION strayed away from the original prompt by interpreting its intended focus as the road, adding the forest element spontaneously, while the KANDINSKY chain continued to interpret the intended focus of the caption as the trucks, producing images which are relatively faithful to the original seed image despite small changes such as the color of the vehicles.

Figure 5 displays a similar comparison between KANDINSKY and STABLE-DIFFUSION, this time captioned with TEXTCAPS, with the former chain breaking after the 12th generated image, and the latter after the 2nd generated image. While the KANDINSKY chain mostly kept the focus on the broccoli, only shifting to focus on the bowl at the end, the STABLE-DIFFUSION chain adds a new element, mushrooms, and quickly makes that the focus of the chain. In these instances, STABLE-DIFFUSION falls further toward fluidity on the faithful \rightarrow fluid scale, while KANDINSKY falls closer to faithful, a fact supported by their KL values.

The specific type of fluidity exhibited in these example chains aligns with the “incorrect attribute binding” glitch phenomenon defined in section 3.2 [Chefer et al., 2023].

Other examples of chain breaks are harder to understand. Unlike the clear patterns of meandering depicted in the chains described earlier, the chain produced by “ground truth” image 0071, using a combination of BLIP and STABLE-DIFFUSION abruptly shifts from “wine” to “bar” between generated images 9 and 10, informing the rest of the chain, which then focuses on beer. At a glance, the 9th and 10th generated images (shown in Figure 6), between which the chain breaks, both look like wine, so the low CLIP and YOLOWORLD similarity score is difficult to understand. However, by using the ResNet152 image classification model and the REX image explanation tool, the reason becomes more clear: the label given for the 9th generated image by ResNet152, from which the REX explanation was created, is “wine”, and a tiny portion of a wineglass highlighted as a sufficient visual explanation [He et al., 2016]. These models recognize “beer” in the 10th image, but produce a much larger visual explanation. This size discrepancy could indicate that the underlying structure of image 10 is more ambiguous than of image 9, requiring an object detector to take into account a larger area of pixels within the image structure in order to determine the most appropriate label. Building on this, one explanation for why some image generators are more creative than others can be surmised: a lack of global cohesiveness within a generated image due to the generation process could produce results



(a) Chain produced using STABLE-DIFFUSION and BLIP.



(b) Chain produced using KANDINSKY and BLIP.

Figure 4: Example chains produced by “ground truth” image 0011, labeled “truck”, where the top left is the “ground truth” image and the rest are generated.

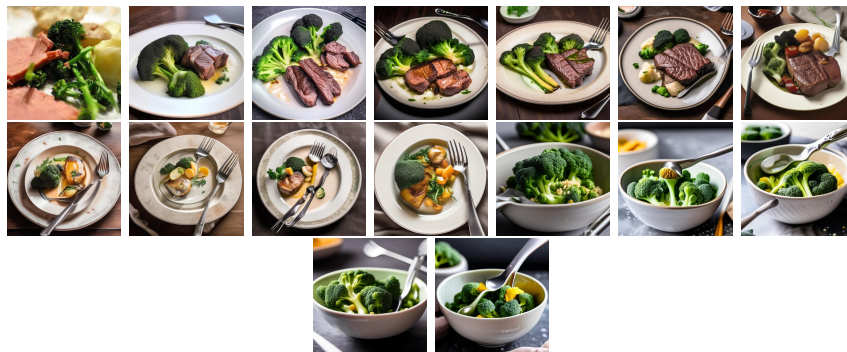
that can straddle multiple class labels and cause shifts in prompt interpretation.

4 Limitations

Our approach comes with a number of limitations. Firstly, the code is quite expensive to run, as it utilizes multiple large models and generates roughly 15000 images per combination. Even using multiple GPUs and not rerunning finished chains, some of the slowest combinations can take over a day to run. In the future, we could optimize our code to resolve this issue. Our dummy chain construction was also constrained to just three common classes found in coco_1000, as finding images for this purpose was somewhat difficult due to a lack of dedicated real-image datasets with labels that match our seed images. Perhaps including more classes would have changed the control group results, and potentially our statistical results. However, given the similarities we observed between the captions produced for different real-world images of simple objects



(a) Chain produced using STABLE-DIFFUSION and TEXTCAPS.



(b) Chain produced using KANDINSKY and TEXTCAPS.

Figure 5: Example chains produced by “ground truth” image 0004, labeled “broccoli”, where the top left is the “ground truth” image and the rest are generated.

like the ones in our seed image dataset, we believe this is unlikely.

Some chains produce breakage results which are difficult to understand: the KANDINSKY BLIP chain for “ground truth” image 0175 breaks between generated images 13 and 14, shown in Figure 7, due to a low object detector similarity score, but despite having different labels ranked as “most important”, both images are visually nearly identical. This makes it difficult to draw conclusions about some data produced by this experiment, although the larger statistical patterns still hold up under scrutiny.

Finally, it is important to acknowledge the impact machine creativity studies could have on human artists. There are already numerous instances of controversial “co-creative” collaborations between human and machine agents [Daniele and Song, 2019]. Research which suggests that models may display autonomously creative behavior could be used in arguments against the importance of fully human-created art. This is not our intention, which is why we have emphasized equal, co-creative collaborations between human artists and AI.

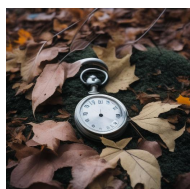


(a) The 9th generated image, captioned “several glasses of wine are lined up on a bar”



(b) The 10th generated image, captioned “four glasses of beer are lined up on a bar”

Figure 6: Two images from a chain created from image 0071 using STABLE-DIFFUSION and BLIP: the image in Figure 6b caused the chain to break, and Figure 6a is the image immediately before it.



(a) The 13th image in the chain.



(b) The 14th image in the chain.

Figure 7: Two images from a chain created from image 0071 using STABLE-DIFFUSION and BLIP: the image in Figure 7b, captioned “a close up of a pocket watch on a moss covered ground”, caused the chain to break; Figure 7a, captioned “there is a pocket watch sitting on the ground surrounded by leaves”, is the image immediately before it.

5 Conclusions

We argue that glitches in image generation could be viewed not as mistakes, but as products of creative semantic interpretation, akin to how humans playing Chinese Whispers may come up with vastly different interpretations of given textual prompts. Our proposed new creativity measure, fluidity, can be quantified through using statistical analysis tools on a series of experiments which measure glitch frequencies in an array of image generators. Placing generators on our scale from maximally fluid to maximally faithful can allow users to choose a generation model based on creative behaviour, in accordance with their intended use case.

References

- Teresa M. Amabile. The social psychology of creativity: A componential conceptualization. *Journal of Personality and Social Psychology*, 45(2):357–376, Aug 1983. doi: 10.1037//0022-3514.45.2.357.
- Harel Berger, Aidan Dakhama, Zishuo Ding, Karine Even-Mendoza, David Kelly, Hector D. Menendez, Rebecca Moussa, and Federica Sarro. Stableyolo: Optimizing image generation for large language models. In *Symposium on Search-Based Software Engineering (SSBSE) 2023*. Springer, December 2023.
- Ricardo Campos, Vítor Mangaravite, Arian Pasquali, Alípio Jorge, Célia Nunes, and Adam Jatowt. Yake! keyword extraction from single documents using multiple local features. *Information Sciences*, 509:257–289, Jan 2020. doi: 10.1016/j.ins.2019.09.013.
- Hila Chefer, Yuval Alaluf, Yael Vinker, Lior Wolf, and Daniel Cohen-Or. Attend-and-excite: Attention-based semantic guidance for text-to-image diffusion models. *ACM Transactions on Graphics*, 42(4):1–10, Jul 2023. doi: 10.1145/3592116.
- Tianheng Cheng, Lin Song, Yixiao Ge, Wenyu Liu, Xinggang Wang, and Ying Shan. Yolo-world: Real-time open-vocabulary object detection. In *Computer Vision and Pattern Recognition Conference*, 2024.
- Hana Chockler, Daniel Kroening, and Youcheng Sun. Explanations for occluded images. In *2021 International Conference on Computer Vision: Proceedings, IEEE/CVF International Conference on Computer Vision (ICCV): Proceedings*. Institute of Electrical and Electronics Engineers Inc., February 2022. doi: 10.1109/ICCV48922.2021.00127.
- Antonio Daniele and Yi-Zhe Song. Ai + art = human. *Proceedings of the 2019 AAAI/ACM Conference on AI, Ethics, and Society*, Jan 2019. doi: 10.1145/3306618.3314233.
- Jennifer Haase and Paul H.P. Hanel. Artificial muses: Generative artificial intelligence chatbots have risen to human-level creativity. *Journal of Creativity*, 33(3):100066, Dec 2023. doi: 10.1016/j.yjoc.2023.100066.
- Kaiming He, Xiangyu Zhang, Shaoqing Ren, and Jian Sun. Deep residual learning for image recognition. In *2016 IEEE Conference on Computer Vision and Pattern Recognition (CVPR)*, pages 770–778, 2016. doi: 10.1109/CVPR.2016.90.
- Yushi Hu, Benlin Liu, Jungo Kasai, Yizhong Wang, Mari Ostendorf, Ranjay Krishna, and Noah A Smith. Tifa: Accurate and interpretable text-to-image faithfulness evaluation with question answering, 2023.
- Alexander Izquierdo. Hugging Face opendalle1.1. <https://huggingface.co/dataautogpt3/OpenDalleV1.1>, 2024.

- Glenn Jocher, Ayush Chaurasia, and Jing Qiu. Ultralytics YOLO, January 2023. URL <https://github.com/ultralytics/ultralytics>.
- James C. Kaufman, Robert J. Sternberg, and Vlad P. Glăveanu. *A Review of Creativity Theories*, page 27–43. Cambridge University Press, 2019.
- Mika Koivisto and Simone Grassini. Best humans still outperform artificial intelligence in a creative divergent thinking task. *Scientific Reports*, 13(1), Sep 2023. doi: 10.1038/s41598-023-40858-3.
- Zhenzhong Lan, Mingda Chen, Sebastian Goodman, Kevin Gimpel, Piyush Sharma, and Radu Soricut. Albert: A lite bert for self-supervised learning of language representations. *Proceedings of the International Conference on Learning Representations*, Apr 2019.
- Junnan Li, Steven Hoi, and Donald Rose. Blip: Bootstrapping language-image pre-training for unified vision-language understanding and generation. Technical report, Salesforce, Jan 2022.
- Md. Khalequzzaman Sarker Likhon. animal_data. <https://www.kaggle.com/datasets/likhon148/animal-data>, 2024.
- Tsung-Yi Lin, Michael Maire, Serge Belongie, James Hays, Pietro Perona, Deva Ramanan, Piotr Dollár, and C. Lawrence Zitnick. Microsoft coco: Common objects in context. *Computer Vision – ECCV 2014*, page 740–755, Sep 2014. doi: 10.1007/978-3-319-10602-1_48.
- Haotian Liu, Chunyuan Li, Qingyang Wu, and Yong Jae Lee. Visual instruction tuning. In *Thirty-seventh Conference on Neural Information Processing Systems*, 2023.
- Henry Berthold Mann and Donald Ransom Whitney. On a test of whether one of two random variables is stochastically larger than the other. *The Annals of Mathematical Statistics*, 18(1):50–60, Mar 1947. doi: 10.1214/aoms/1177730491.
- Jonas Oppenlaender. The creativity of text-to-image generation. *Proceedings of the 25th International Academic Mindtrek Conference*, page 192–202, Nov 2022. doi: 10.1145/3569219.3569352.
- Alec Radford, Jong Wook Kim, Chris Hallacy, Aditya Ramesh, Gabriel Goh, Sandhini Agarwal, Girish Sastry, Amanda Askell, Pamela Mishkin, Jack Clark, and et al. Learning transferable visual models from natural language supervision. In *Proceedings of the International Conference on Machine Learning 2021*, Jun 2021. doi: 10.48550/arXiv.2103.00020.
- Anton Razhigaev, Arseniy Shakhmatov, Anastasia Maltseva, Vladimir Arkhipkin, Igor Pavlov, Ilya Ryabov, Angelina Kuts, Alexander Panchenko, Andrey Kuznetsov, and Denis Dimitrov. Kandinsky: An improved text-to-image synthesis with image prior and latent diffusion. In Yansong Feng and Els Lefever,

- editors, *Proceedings of the 2023 Conference on Empirical Methods in Natural Language Processing: System Demonstrations*, pages 286–295. Association for Computational Linguistics, Dec 2023. doi: 10.18653/v1/2023.emnlp-demo.25.
- Nils Reimers and Iryna Gurevych. Sentence-bert: Sentence embeddings using siamese bert-networks. In *Proceedings of the 2019 Conference on Empirical Methods in Natural Language Processing and the 9th International Joint Conference on Natural Language Processing (EMNLP-IJCNLP)*, Nov 2019. doi: 10.18653/v1/d19-1410.
- Robin Rombach, Andreas Blattmann, Dominik Lorenz, Patrick Esser, and Björn Ommer. High-resolution image synthesis with latent diffusion models. *2022 IEEE/CVF Conference on Computer Vision and Pattern Recognition (CVPR)*, pages 10674–10685, 2021.
- Stuart Rose, Dave Engel, Nick Cramer, and Wendy Cowley. Automatic keyword extraction from individual documents. *Text Mining*, page 1–20, Mar 2010. doi: 10.1002/9780470689646.ch1.
- Axel Sauer, Dominik Lorenz, Andreas Blattmann, and Robin Rombach. Adversarial diffusion distillation. *ArXiv*, abs/2311.17042, 2023.
- Philip Sedgwick. Multiple significance tests: the bonferroni correction. *BMJ (online)*, 344:e509–e509, 01 2012. doi: 10.1136/bmj.e509.
- Samuel Sanford Shapiro and Martin Bradbury Wilk. An analysis of variance test for normality (complete samples). *Biometrika*, 52(3/4):591, Dec 1965. doi: 10.2307/2333709.
- Tony Veale, F. Amílcar Cardoso, and Rafael Pérez y Pérez. *Systematizing Creativity: A Computational View*, pages 1–19. Springer International Publishing, Cham, 2019. ISBN 978-3-319-43610-4. doi: 10.1007/978-3-319-43610-4_1. URL https://doi.org/10.1007/978-3-319-43610-4_1.
- Pauli Virtanen, Ralf Gommers, Travis E. Oliphant, Matt Haberland, Tyler Reddy, David Cournapeau, Evgeni Burovski, Pearu Peterson, Warren Weckesser, Jonathan Bright, Stéfan J. van der Walt, Matthew Brett, Joshua Wilson, K. Jarrod Millman, Nikolay Mayorov, Andrew R. J. Nelson, Eric Jones, Robert Kern, Eric Larson, C J Carey, İlhan Polat, Yu Feng, Eric W. Moore, Jake VanderPlas, Denis Laxalde, Josef Perktold, Robert Cimrman, Ian Henriksen, E. A. Quintero, Charles R. Harris, Anne M. Archibald, Antônio H. Ribeiro, Fabian Pedregosa, Paul van Mulbregt, and SciPy 1.0 Contributors. SciPy 1.0: Fundamental Algorithms for Scientific Computing in Python. *Nature Methods*, 17:261–272, 2020. doi: 10.1038/s41592-019-0686-2.
- Jianfeng Wang, Zhengyuan Yang, Xiaowei Hu, Linjie Li, Kevin Lin, Zhe Gan, Zicheng Liu, Ce Liu, and Lijuan Wang. Git: A generative image-to-text transformer for vision and language. Technical report, Microsoft, May 2022.

Roosa Wingström, Johanna Hautala, and Riina Lundman. Redefining creativity in the era of ai? perspectives of computer scientists and new media artists. *Creativity Research Journal*, 36(2):177–193, Aug 2022. doi: 10.1080/10400419.2022.2107850.

A Technical Appendices

Algorithm 1 Pseudo-code for the LABEL_SIM algorithm

```

init_img_labels
curr_img_labels
similarity  $\leftarrow$  0
for  $l$  in init_img_labels do
  if  $l$  in  $m$  then
    similarity  $\leftarrow$  similarity + 1
  else
    maxsim  $\leftarrow$  0
    for each  $l_2$  in curr_img_labels do
      if  $maxsim \leq S - BERTScore(l, l_2)$  then
        maxsim  $\leftarrow S - BERTScore(l, l_2)$ 
      end if
    end for
    similarity  $\leftarrow$  similarity + maxsim
  end if
end for

```

Examples of experiments using LLAVA for image 0045 from the ground truth dataset:

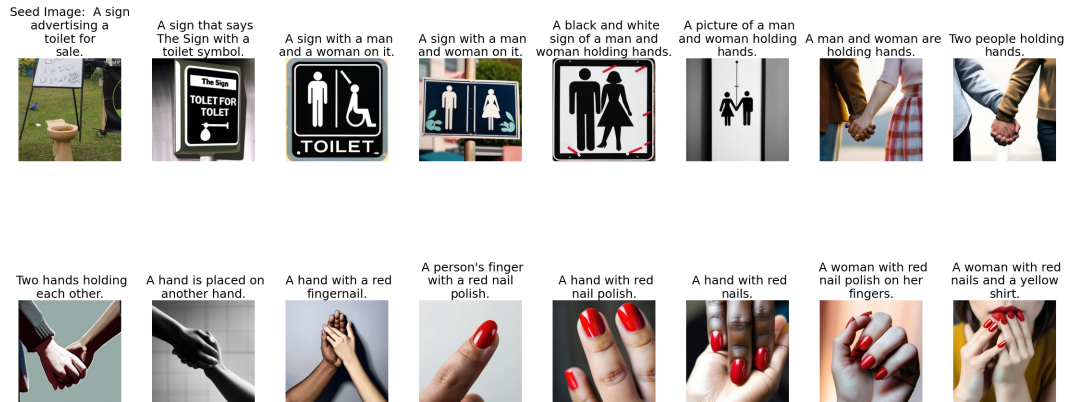


Table 1: The chain constructed using OPENDALLE + LLAVA for image 0045

The breakdown of the scores based on image and caption comparison for the chain shown in Figure 1.

Algorithm 2 Pseudo-code for our breakage algorithm

```

initial_img
current_img
initial_img_labels
current_img_labels
initial_caption
current_caption
breakage  $\leftarrow$  False
if  $CLIP_{score}(initial\_img, current\_img) < 20$  then
    breakage  $\leftarrow$  True
end if
if  $BERT_{score}(initial\_cap, current\_cap) < 0.5$  &
 $S-BERT_{score}(initial\_cap, current\_cap) < 0.5$  then
    breakage  $\leftarrow$  True
end if
if  $LABEL\_SIM(initial\_img\_labels, current\_img\_labels) < 0.5$  then
    breakage  $\leftarrow$  True
end if

```

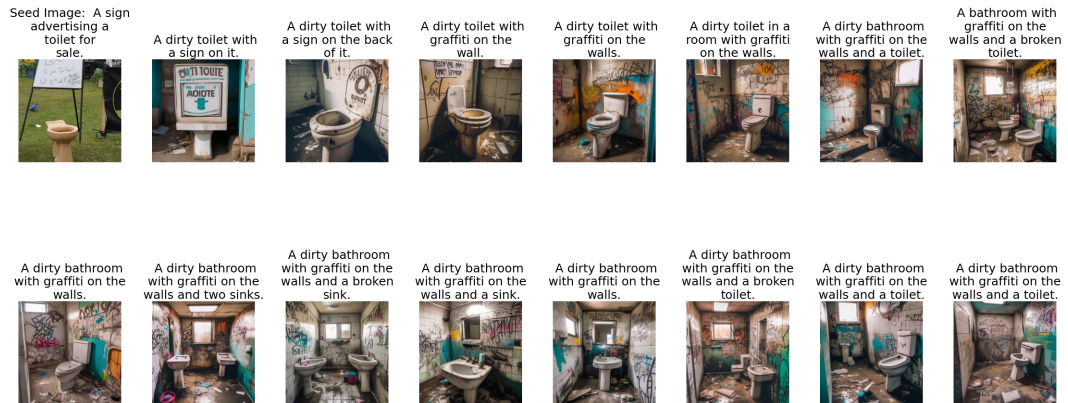


Table 2: The chain constructed using KANDINSKY + LLAVA for image 0045

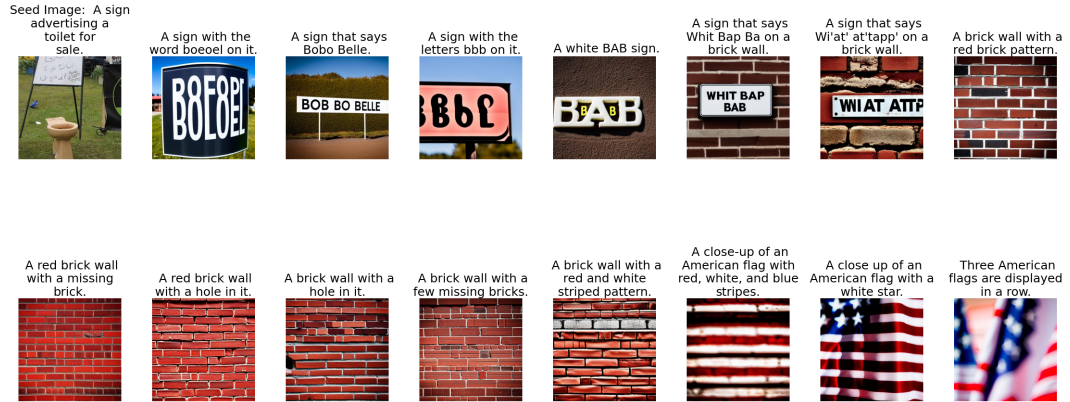


Table 3: The chain constructed using STABLE-DIFFUSION + LLAVA for image 0045



Table 4: The chain constructed using SDXL-TURBO + LLAVA for image 0045

Table 5: The scores for image comparisons for img 0045 using LLAVA and OPENDALLE

	Clip Score	CLIP Label	Similarity of CLIP	YOLO Label	Similarity of YOLO	Broken
0	21.7736	['sign advertising']	1	['sign advertising']	1	False
1	27.167	['toilet symbol']	0.123	['sign']	0.664	False
2	24.0346	['sign']	0.664	[]	0	False
3	24.4452	['sign']	0.664	[]	0	False
4	25.0439	['holding hands']	0.144	[]	0	True
5	23.9566	['holding hands']	0.144	[]	0	True
6	23.6537	['holding hands']	0.144	[]	0	True
7	24.1034	['holding hands']	0.144	[]	0	True
8	22.6222	['hands holding']	0.133	['person']	0.125	True
9	23.9779	['hand']	0.126	['person']	0.125	True
10	23.088	['hand']	0.126	['person']	0.125	True
11	23.1896	['nail polish']	0.113	['person']	0.125	True
12	21.3481	['nail polish']	0.113	['person']	0.125	True
13	20.1922	['red nails']	0.085	['person']	0.125	True
14	20.9572	['red nail']	0.045	['person']	0.125	True
15	18.894	['red']	0.091	['person']	0.125	True

Table 6: The scores for initial and current caption textual comparisons for img 0045, using LLAVA and OPENDALLE

	Caption	CLIP Score	BERT Score	S-BERT Score	Broken
0	A sign advertising a toilet for sale.	21.7736	1	1	False
1	A sign that says The Sign with a toilet symbol.	27.167	0.762	0.789	False
2	A sign with a man and a woman on it.	24.0346	0.679	0.431	False
3	A sign with a man and woman on it.	24.4452	0.677	0.447	False
4	A black and white sign of a man and woman holding hands.	25.0439	0.621	0.248	True
5	A picture of a man and woman holding hands.	23.9566	0.615	0.108	True
6	A man and woman are holding hands.	23.6537	0.573	0.038	True
7	Two people holding hands.	24.1034	0.598	0.102	True
8	Two hands holding each other.	22.6222	0.538	0.104	True
9	A hand is placed on another hand.	23.9779	0.542	0.177	True
10	A hand with a red fingernail.	23.088	0.672	0.196	True
11	A person’s finger with a red nail polish.	23.1896	0.63	0.145	True
12	A hand with red nail polish.	21.3481	0.65	0.209	True
13	A hand with red nails.	20.1922	0.682	0.174	True
14	A woman with red nail polish on her fingers.	20.9572	0.61	0.053	True
15	A woman with red nails and a yellow shirt.	18.894	0.624	0.073	True

Table 7: Statistics for Frequency Distributions for Each Combination

Model	Caption	KL Divergence	Mean Chain Length	Skewness	P-Value
KANDINSKY	BLIP	0.711418	7.399	3.85383	0.000116283
KANDINSKY	TEXTCAPS	0.575388	6.496	3.29603	0.000980611
KANDINSKY	LLAVA	0.945868	8.776	4.41298	1.01959e-05
OPENDALLE	BLIP	0.44288	6.728	3.43983	0.00058209
OPENDALLE	TEXTCAPS	0.381594	5.309	2.37619	0.0174923
OPENDALLE	LLAVA	0.576568	7.366	3.92607	8.63434e-05
STABLE-DIFFUSION	BLIP	0.410231	5.099	2.58584	0.00971408
STABLE-DIFFUSION	TEXTCAPS	0.458674	4.384	2.82806	0.00468312
STABLE-DIFFUSION	LLAVA	0.470352	5.679	2.69947	0.0069451
SDXL-TURBO	BLIP	0.685981	7.949	4.24887	2.14849e-05
SDXL-TURBO	TEXTCAPS	0.603585	7.024	3.67724	0.000235768
SDXL-TURBO	LLAVA	0.78107	8.331	4.32471	1.52734e-05

Table 8: Statistics for Frequency Distributions for Control Combinations

Model	Caption	KL Divergence	Mean Chain Length	Skewness	P-Value
Control	BLIP	2.169674	13.523	4.90856	9.174705e-07
Control	TEXTCAPS	2.078700	12.777	4.86619	1.13773e-06
Control	LLAVA	2.180563	12.619	4.75709	1.96402e-05

Table 9: Mann-Whitney U Comparisons for Control + Caption Gen & Image + Caption Gen Combinations

Image Generator 1	Caption Generator	p-value
OPENDALLE	BLIP	0.0005
OPENDALLE	LLAVA	0.0004
OPENDALLE	TEXTCAPS	0.0006
KANDINSKY	BLIP	0.0012
KANDINSKY	LLAVA	0.0005
KANDINSKY	TEXTCAPS	0.0011
STABLE-DIFFUSION	BLIP	0.0005
STABLE-DIFFUSION	LLAVA	0.0003
STABLE-DIFFUSION	TEXTCAPS	0.0009
SDXL-TURBO	BLIP	0.0008
SDXL-TURBO	LLAVA	0.0004
SDXL-TURBO	TEXTCAPS	0.0012

Table 10: Mann-Whitney U Comparisons for Image Generators

Caption Generator	Image Generator 1	Image Generator 2	p-value	
	BLIP	KANDINSKY	OPENDALLE	0.2538
	BLIP	KANDINSKY	STABLE-DIFFUSION	0.4426
	BLIP	KANDINSKY	SDXL-TURBO	0.7086
	BLIP	SDXL-TURBO	OPENDALLE	0.5067
	BLIP	SDXL-TURBO	STABLE-DIFFUSION	0.5894
	BLIP	STABLE-DIFFUSION	OPENDALLE	0.7874
	LLAVA	KANDINSKY	OPENDALLE	0.2447
	LLAVA	KANDINSKY	STABLE-DIFFUSION	0.2537
	LLAVA	KANDINSKY	SDXL-TURBO	0.4550
	LLAVA	SDXL-TURBO	OPENDALLE	0.5609
	LLAVA	SDXL-TURBO	STABLE-DIFFUSION	0.5473
	LLAVA	STABLE-DIFFUSION	OPENDALLE	0.9503
	TEXTCAPS	KANDINSKY	OPENDALLE	0.5894
	TEXTCAPS	KANDINSKY	STABLE-DIFFUSION	0.8845
	TEXTCAPS	KANDINSKY	SDXL-TURBO	1.0
	TEXTCAPS	SDXL-TURBO	OPENDALLE	0.5066
	TEXTCAPS	SDXL-TURBO	STABLE-DIFFUSION	0.8519
	TEXTCAPS	STABLE-DIFFUSION	OPENDALLE	0.7398

Table 11: Mann-Whitney U Comparisons for Caption Generators

Image Generator	Caption Generator 1	Caption Generator 2	p-value	
	CONTROL	BLIP	LLAVA	0.8736
	CONTROL	BLIP	TEXTCAPS	0.5180
	CONTROL	LLAVA	TEXTCAPS	0.6891
	OPENDALLE	BLIP	LLAVA	0.5753
	OPENDALLE	BLIP	TEXTCAPS	0.9504
	OPENDALLE	LLAVA	TEXTCAPS	0.7872
	KANDINSKY	BLIP	LLAVA	0.5335
	KANDINSKY	BLIP	TEXTCAPS	0.8194
	KANDINSKY	LLAVA	TEXTCAPS	0.4426
	STABLE-DIFFUSION	BLIP	LLAVA	0.8194
	STABLE-DIFFUSION	BLIP	TEXTCAPS	0.8194
	STABLE-DIFFUSION	LLAVA	TEXTCAPS	1.0
	SDXL-TURBO	BLIP	LLAVA	0.8033
	SDXL-TURBO	BLIP	TEXTCAPS	0.9338
	SDXL-TURBO	LLAVA	TEXTCAPS	0.6781